Electronic Supplementary Material (ESI) for Energy & Environmental Science.
This journal is © The Royal Society of Chemistry 2014

Electronic supplementary information for:

Self-powered fully-flexible light-emitting system enabled by flexible energy harvester

Chang Kyu Jeong,‡[a] Kwi-Il Park,‡[a] Jung Hwan Son,‡[a] Geon-Tae Hwang,[a] Seung Hyun Lee,[a] Dae Yong Park,[a] Han Eol Lee,[a] Hwan Keon Lee,[a] Myunghwan Byun,[a] and Keon Jae Lee*[a]

[a]Department of Materials Science and Engineering, Korea Advanced Institute of Science and Technology (KAIST), 291 Daehak-ro, Yuseong-gu, Daejeon 305-701, Republic of Korea

‡These authors contributed equally to this work.

This PDF file includes:

Fig. S1 to S16

Calculation for the laser penetration depth and heat diffusion length of the PZT

Calculation for the mechanical neutral plane and the effective strain in PZT thin film

Calculation for the energy conversion efficiency

Other Supplementary Information for this manuscript

Video S1

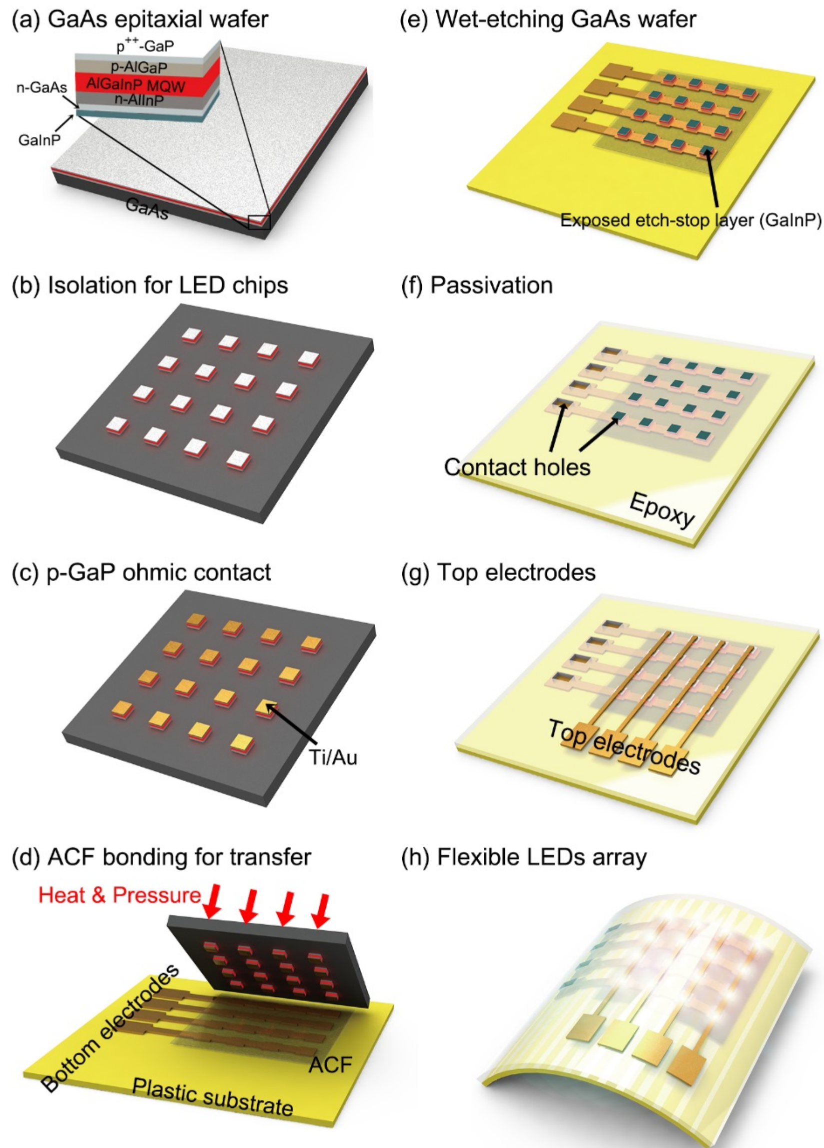

Fig. S1. Schematics of the fabrication steps for f-VLEDs. (a) Preparation of GaAs epitaxial wafer. The details of epitaxial layers on the GaAs mother substrate are depicted in Fig. S2†. (b) Microscale LED chips are isolated by photolithography and ICP-RIE dry etching. (c) p-GaP ohmic contact is formed with Ti/Au metal layers. (d) To attach the LED chips onto a bottom electrodes-patterned plastic substrate, ACF bonding is conducted by heat and pressure. (e) Removal of the GaAs mother wafer using ammonia-based etchant. The GaInP layer (dry etch-stop layer) become an upward part because the LED chips are flipped over. (f) Whole area is passivated by SU-8 epoxy except for the parts of LED chips and bottom electrodes contact regions. (g) Top electrodes are defined by photolithography. (h) Illustration of the final f-VLEDs array.

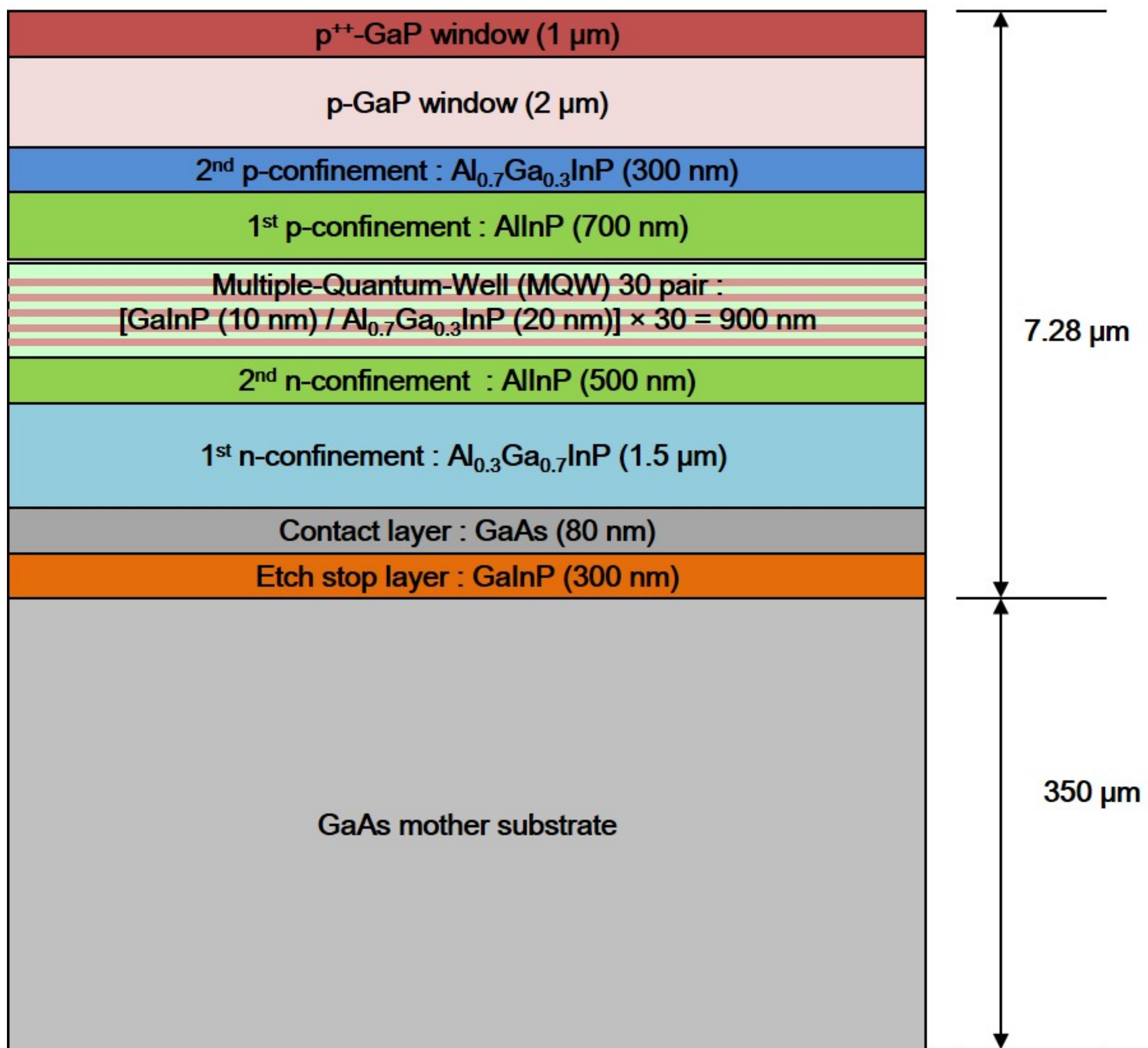

Fig. S2. Detail structure of GaAs epitaxial wafer. The wafer is prepared by Kodenshi Co.

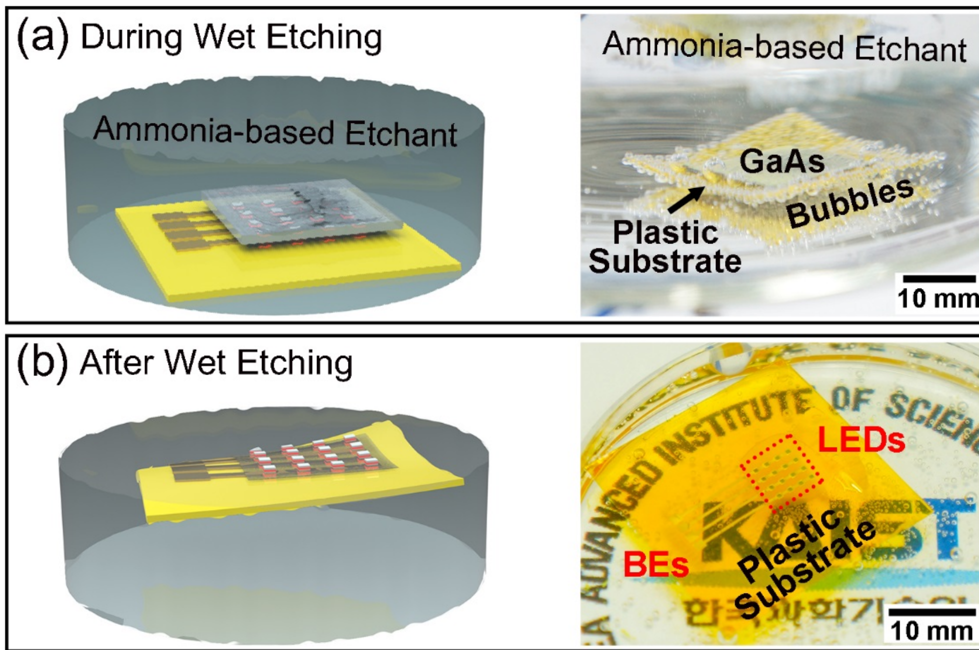

Fig. S3. Wet etching process for the removal of GaAs mother substrate. (a) GaAs wafer with LED chips bonded on a plastic substrate by the ACF sinks into the specific ammonia-based etchant. The etchant solution is made of NH_4OH and H_2O_2 (volume ratio of 1:6). The processing temperature is 45 °C. (b) The GaAs mother substrate is completely removed after about 1 h. The f-VLEDs array spontaneously floats on the surface of the etchant solution.

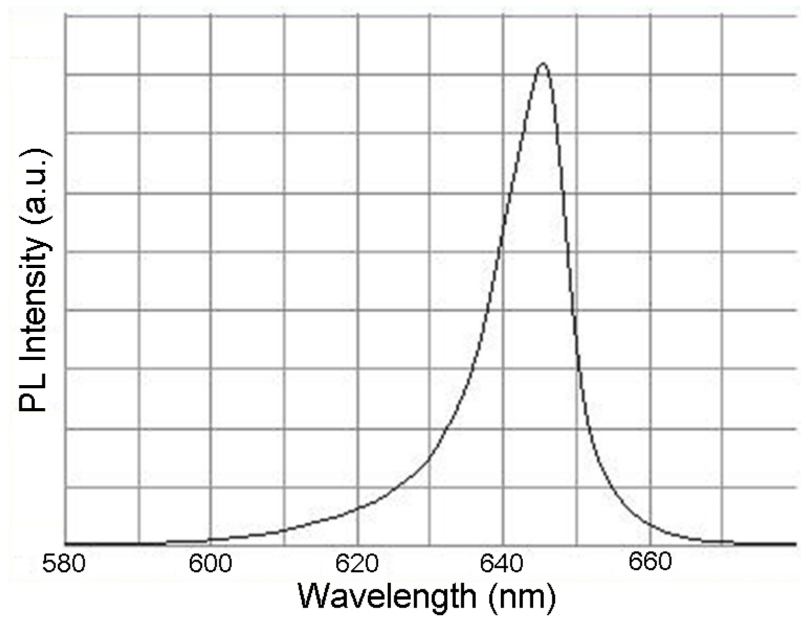

Fig. S4. PL spectrum of the epitaxial layers on GaAs wafer.

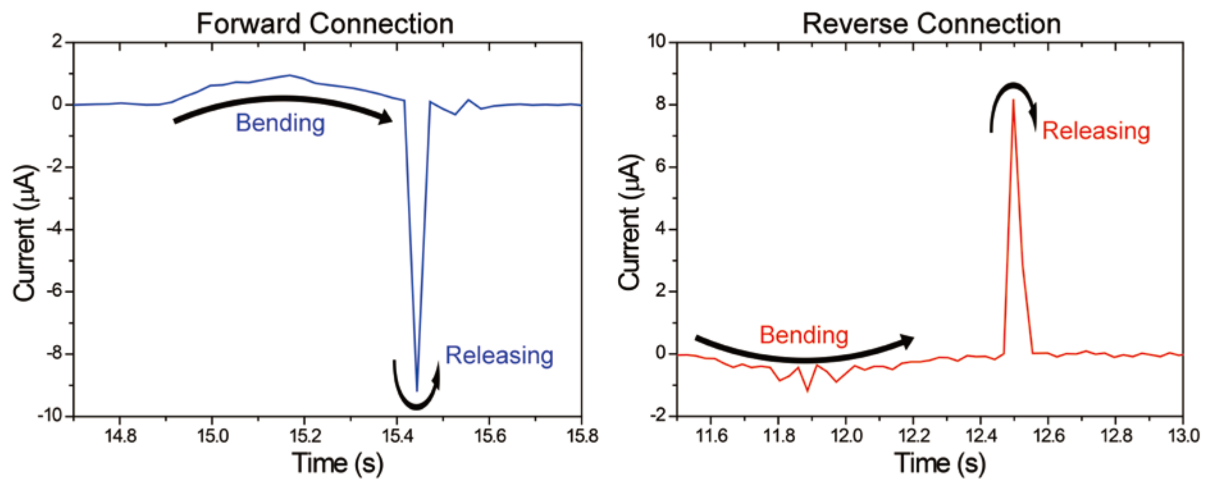

Fig. S5. Magnified current signals generated from the PZT thin film energy harvester by finger flicking. Bending the flexible energy harvester by fingers generates a low and broad current signal whereas releasing the energy harvester can produce a high and sharp current peak due to the discrepancies of the strain rate between the bending/releasing motions inevitably resulting from finger flicking. Note that the total amount of flowing charges (current × time) have to be maintained; therefore, the current level become higher as the strain rate occurs faster. The FWHM of generated current signals by releasing is about 50 ms.

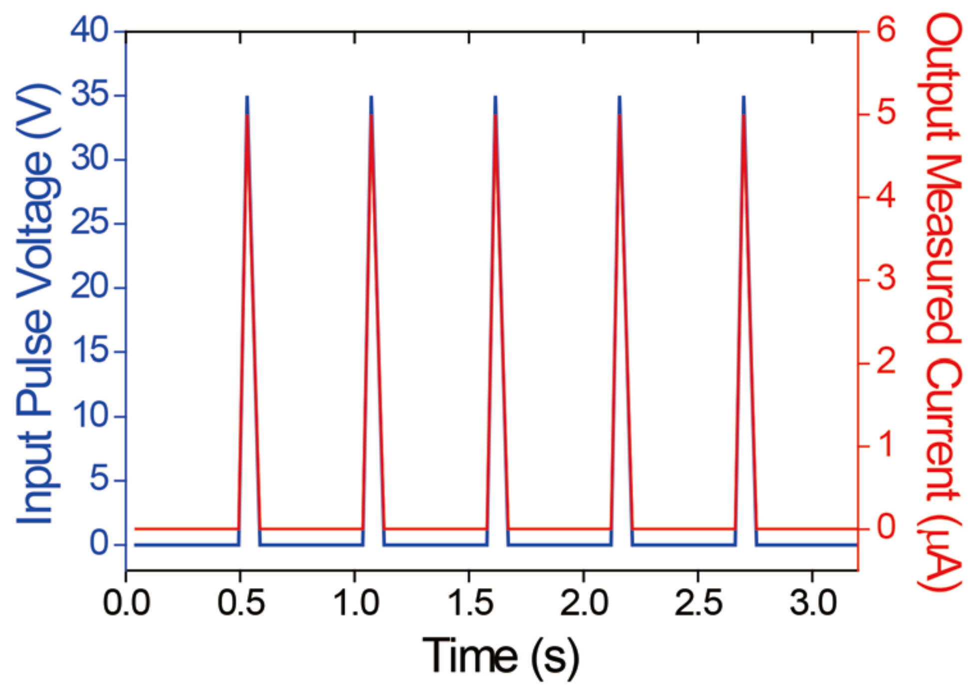

Fig. S6. Pulsed input voltage signals (FWHM of 50 ms corresponding to generated signals of energy harvester) can operate the f-VLEDs.

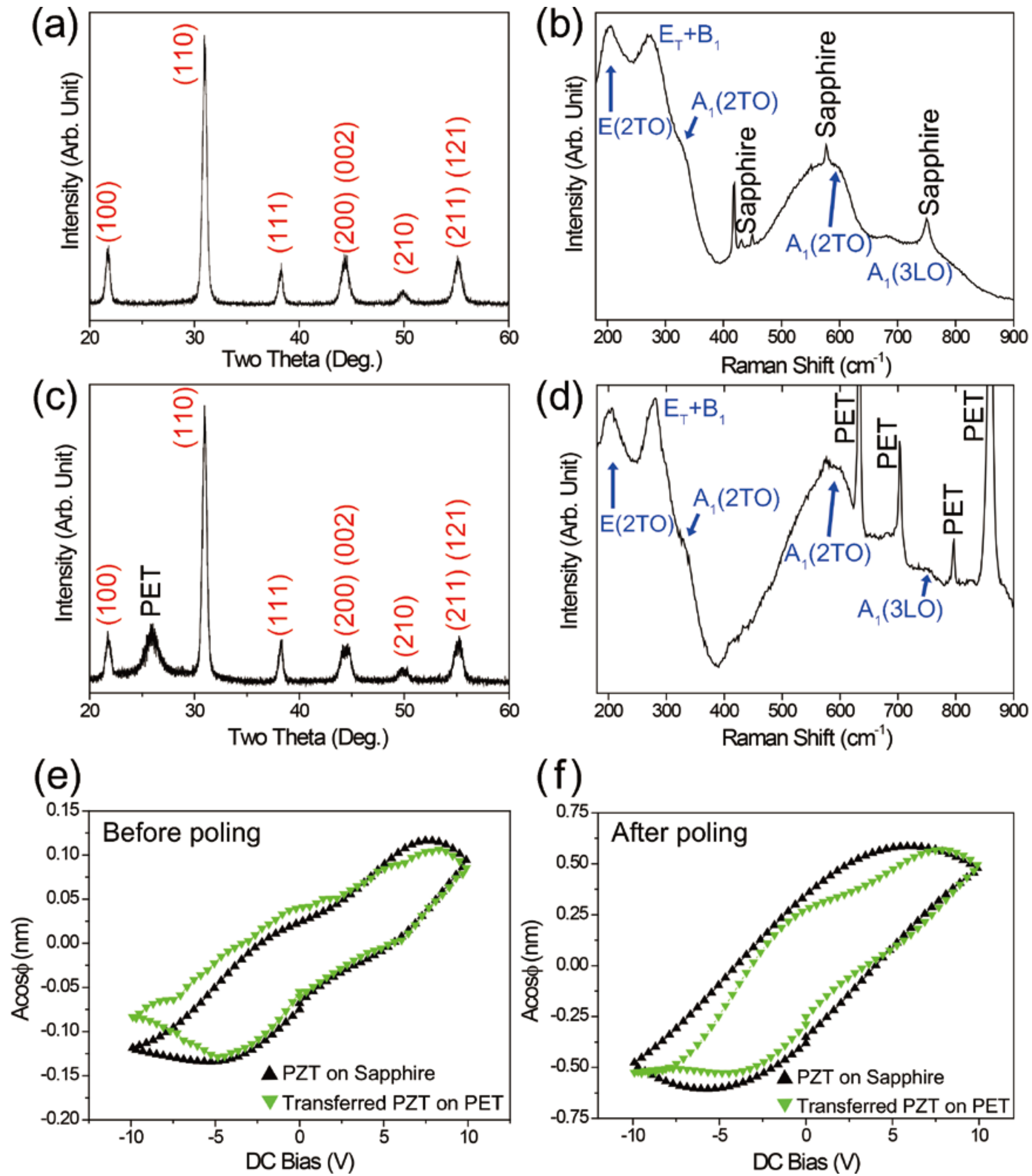

Fig. S7. XRD patterns and Raman spectroscopy data of the PZT thin film (a,b) before and (c,d) after LLO process, respectively. XRD analyses were performed by the theta fixed-two theta scan method to maximize the peaks of PZT film and minimize substrate peaks. (e) Before and (f) after the poling process, PFM hysteresis loops of the PZT thin film on a sapphire wafer and the transferred PZT thin film on a PET plastic substrate. Without poling, the effective piezoelectric coefficient (d_{33}) of the PZT thin film was about 10-15 pm V^{-1}. After the poling at 120 °C under an electric field of 100 kV cm^{-1} for about 6 h, d_{33} increased to 50-60 pm V^{-1} which well corresponds with the previously reported values of PZT thin films (40-110 pm/V).[1-4]

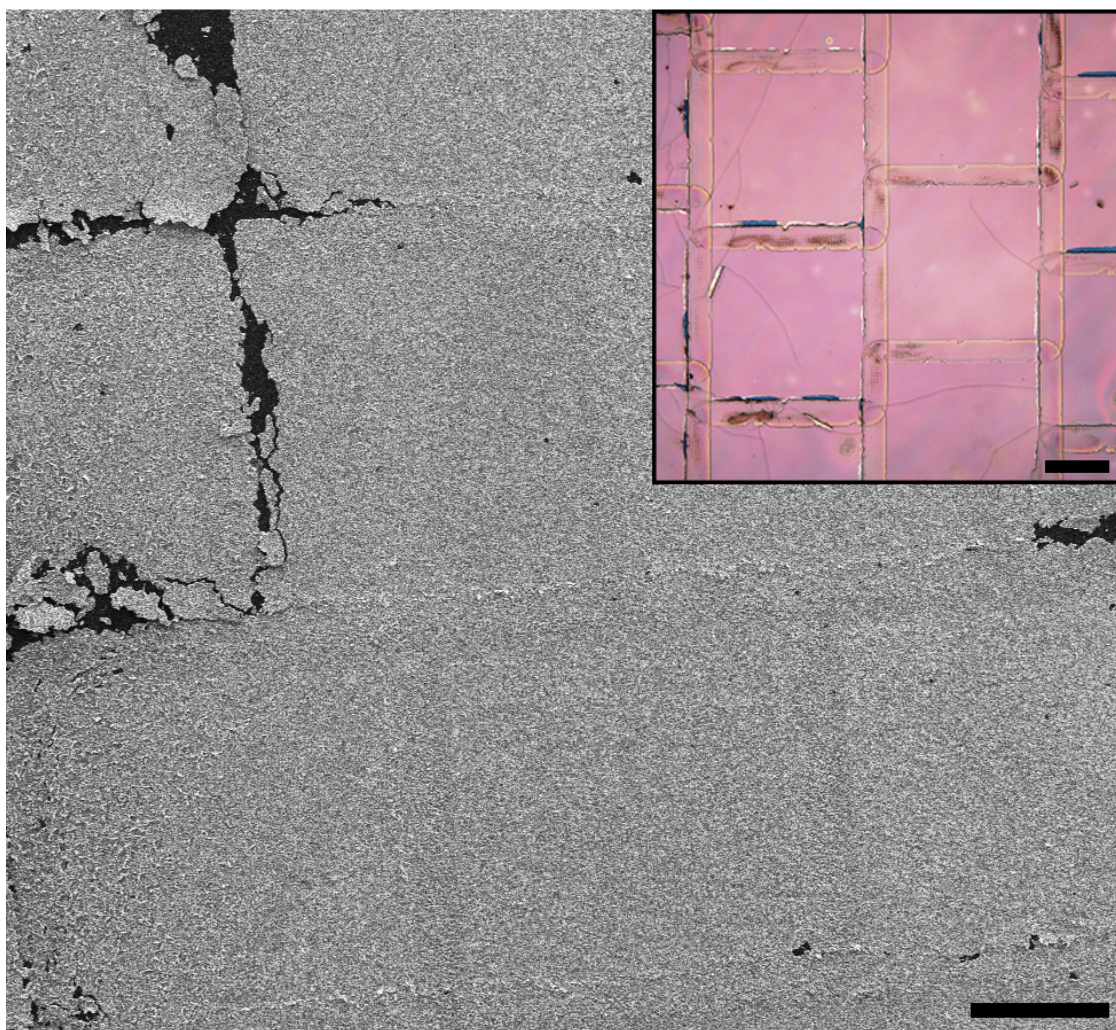

Fig. S8. SEM image and optical micrograph (inset) of the PZT thin film transferred to a PET substrate by the LLO process using laser of higher energy density (500 mJ cm^{-1}) than optimised energy density (420 mJ cm^{-2}). Scale bars, 200 μm.

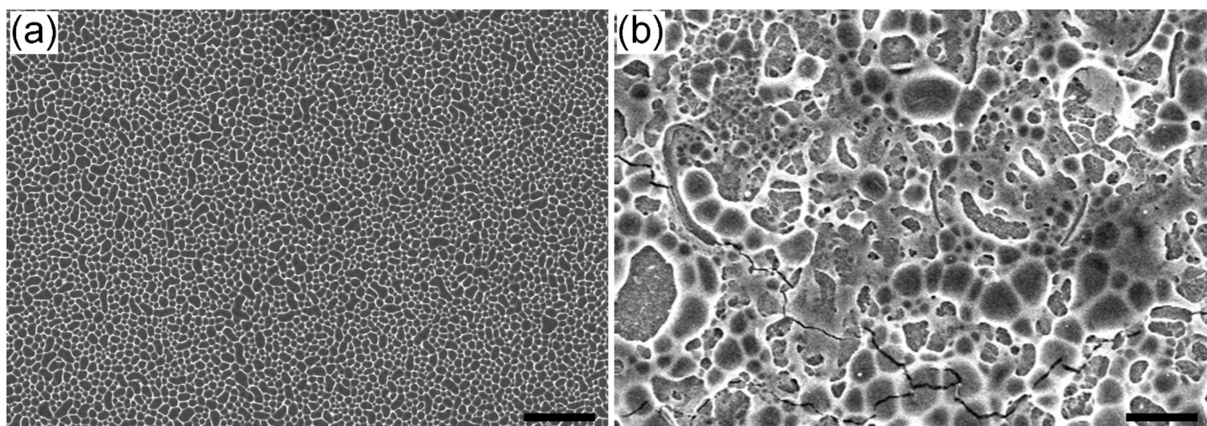

Fig. S9. Magnified SEM images of surfaces of the PZT thin films transferred to a PET substrate by the LLO process using laser with (a) optimised energy density (420 mJ cm^{-2}) and (b) excessively high energy density (500 mJ cm^{-1}) which is a non-optimum failure condition. Scale bars, 3 μm.

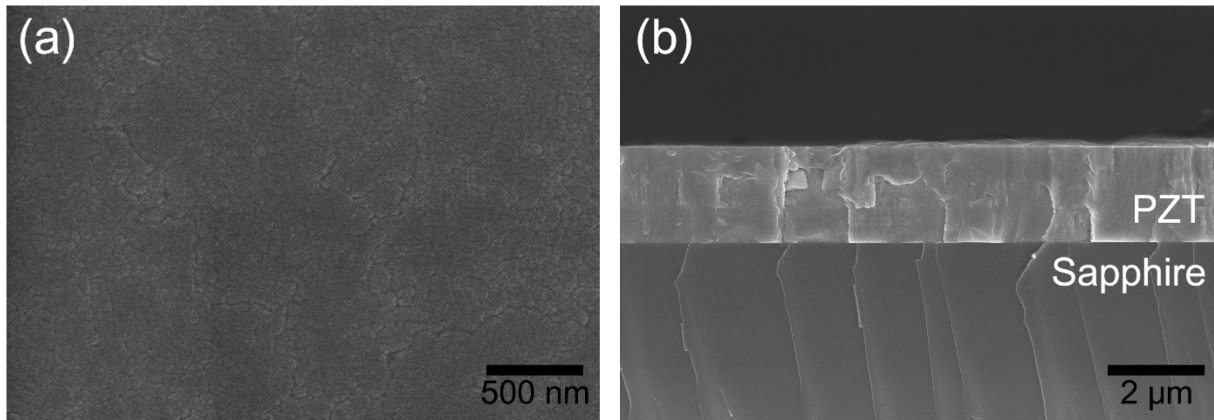

Fig. S10. SEM images of (a) top-view and (b) cross-sectional view of PZT thin film before LLO process, respectively.

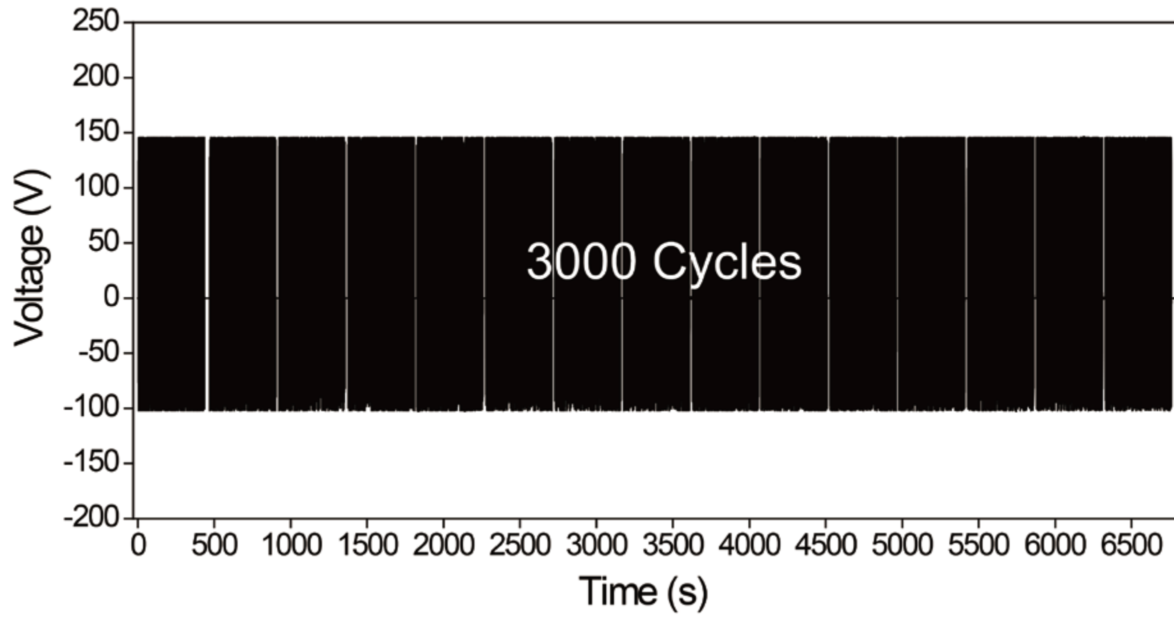

Fig. S11. The durability and stability test of PZT thin film energy harvester with 3000 cyclic bending deformation. The PZT thin film energy harvester stably generated output voltage signals during the repeated bending test.

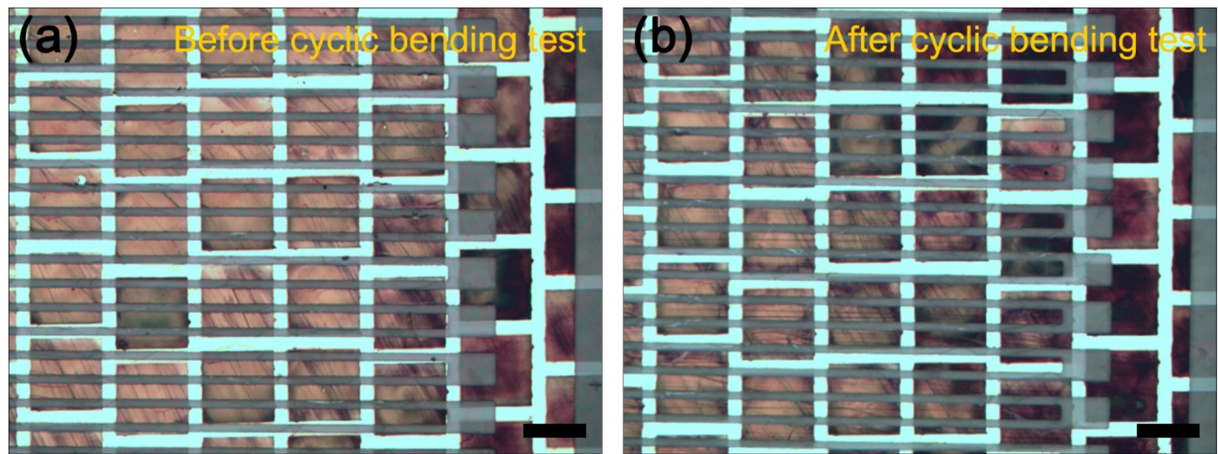

Fig. S12. Optical microscopy images of PZT thin film energy harvester with the SU-8 passivation layer (a) before and (b) after 3000 cyclic bending test. There is no crack after the durability test. Scale bars, 300 μm.

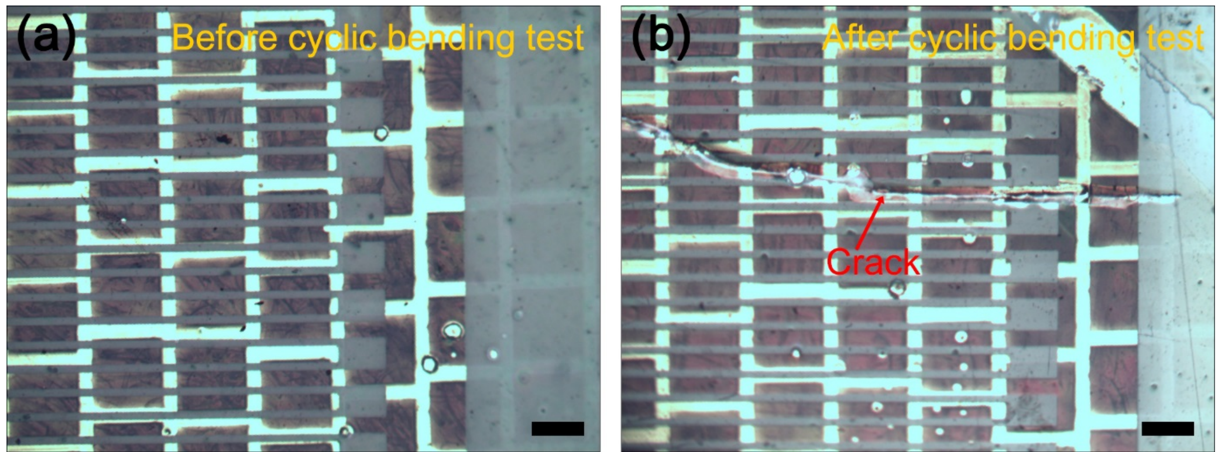

Fig. S13. Optical microscopy images of PZT thin film energy harvester without the passivation layer (a) before and (b) after 10 cyclic bending test. There is a significant crack after the bending test. Scale bars, 300 μm.

Calculation for the laser penetration depth and heat diffusion length of the PZT

The penetration depth (*d*) and heat diffusion length (*x*) of the laser are defined as below,

$$d = \frac{1}{\alpha} = \frac{\lambda}{4\pi k_e}$$

$$x = \sqrt{2Dt} = \sqrt{2\left(\frac{k}{C_p \rho}\right)t}$$

where α is the optical absorption coefficient, λ is the wavelength of laser, k_e is the extinction coefficient, D is the heat diffusivity, C_p is the specific heat capacity, ρ is the density, k is thermal conductivity, and t is the laser pulse duration time. As calculated from above equations, the penetration depth and heat diffusion length of the PZT were estimated as 35.7 nm and 209 nm, respectively, assuming $t = 30$ ns, $\lambda = 308$ nm, $\rho = 7.97 \times 10^3$ kg/m^3, $C_p = 360$ J/kg·K, $\alpha = 2.8 \times 10^5$ cm^{-1}, and $k = 2.1$ W/mK.

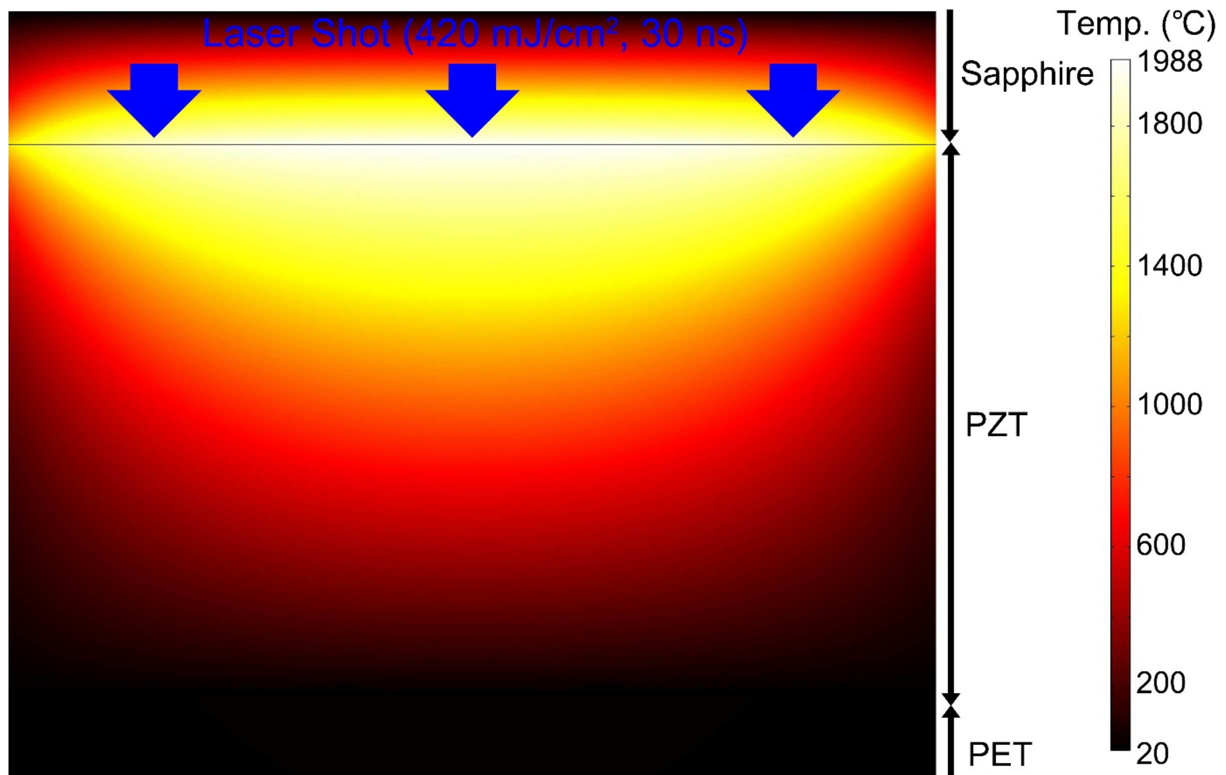

Fig. S14. Finite element analysis (FEA)-based COMSOL static simulation result showing the temperature distribution in the situation that energy density of 420 mJ cm^{-2} is injected to the interface between the sapphire wafer and the PZT thin film. Through this computer simulation, we found that the interfacial temperature reached approximately 2000 °C, which was high enough to locally melt down the interfacial PZT layer (The sintering temperature of PZT is above 1300 °C). On the basis of materials kinetics and dynamics as described in the above equations, the interface can be the only place affected by the laser due to highly-restricted heat diffusion caused by the short laser duration time (~30 ns).

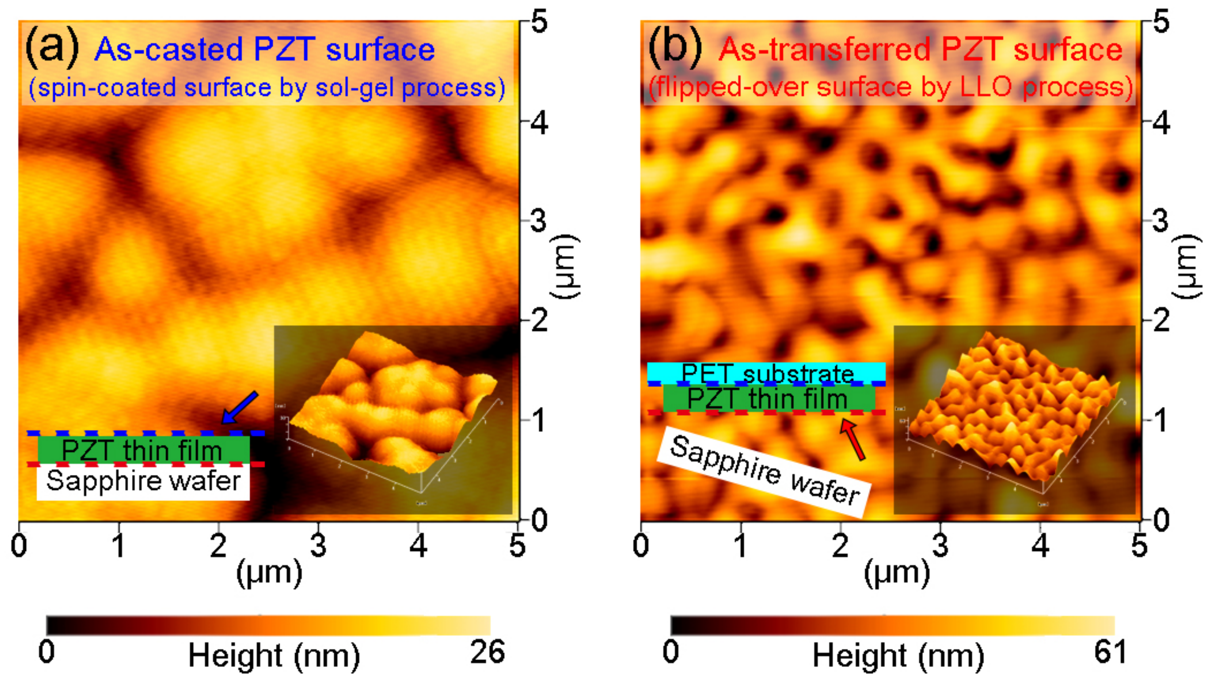

Fig. S15. Atomic force microscopy (AFM) analyses showing surface morphology and roughness. Surface area is fixed as 5 μm × 5 μm. (a) AFM image of PZT surface deposited by sol-gel method on a sapphire wafer. The root mean square (RMS) value is 4.61 nm. (b) AFM image of PZT surface transferred onto PET substrate by the LLO process using XeCl excimer laser (optimum energy density of 420 mJ cm^{-2}). The RMS value is 8.73 nm. The nanoscale bubbled structure is also shown in this image like the SEM image in Fig. S9a. Note that the PZT thin film is flipped over during the LLO transfer process, as clarified by the blue and red dotted lines and arrows in each bottom-left inset schematic. Namely, the exposed PZT surfaces after and before the LLO process are originally opposite-side surfaces.

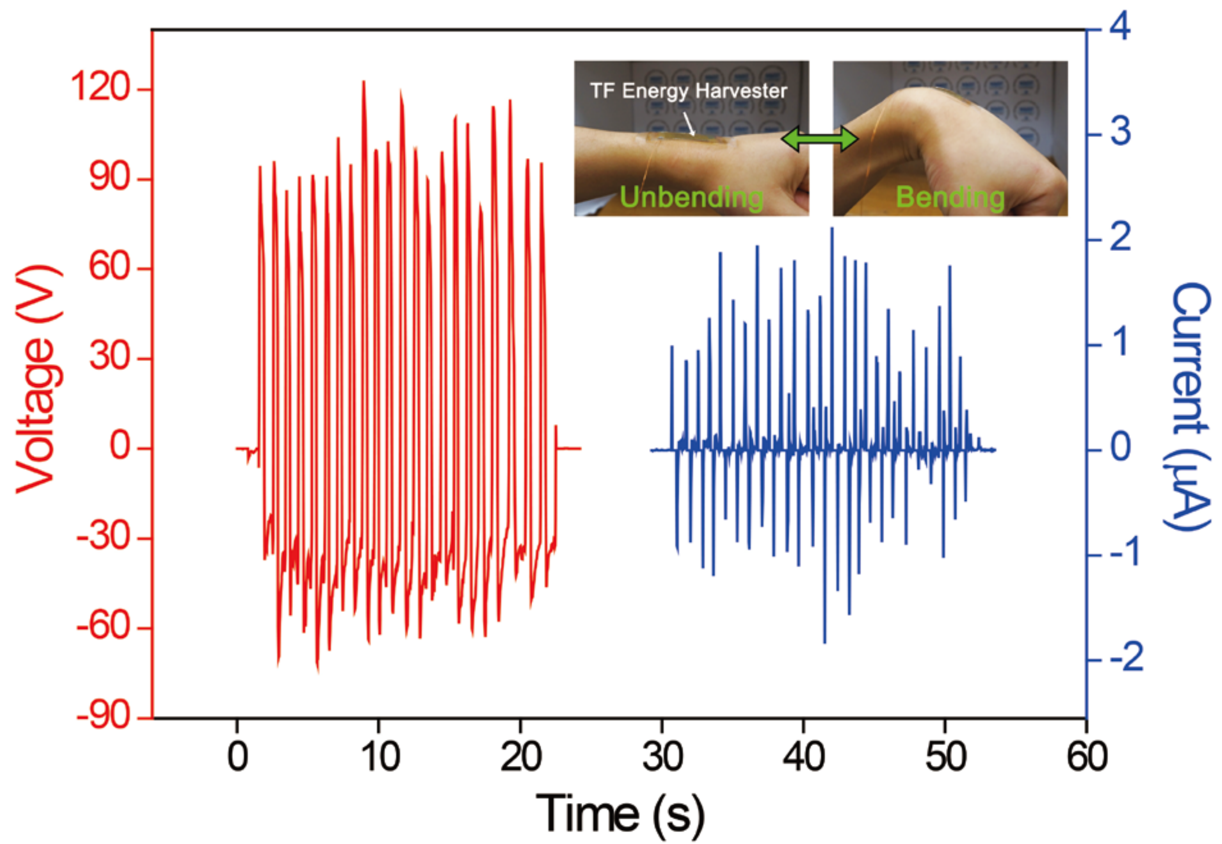

Fig. S16. The generated voltage and current output by the PZT thin film energy harvester conformally attached on a human wrist. These produced signals are comparable to the output of the energy harvester by the bending machine.

Calculation for the mechanical neutral plane and the effective strain in PZT thin film

The distance between the mechanical neutral plane and the top surface can be calculated as the following equation

$$h_{\text{neutral}} = \frac{\sum_{i=1}^{N}\left\{\overline{Y}_i t_i \left(\sum_{j=1}^{i} t_j - \frac{t_i}{2}\right)\right\}}{\sum_{i-1}^{N} \overline{Y}_i t_i}$$

Where N is the total number of layers, t_i is the thickness of the ith layer (from the top), and is $\overline{Y}_i = Y_i/(1-\upsilon_i^2)$ is defined as effective Young's modulus (Y_i ≡ absolute Young's modulus and υ_i ≡ Poisson's ratio of the ith layer). For the system of PZT thin film energy harvester, the elastic properties and thicknesses are (1) $Y_{\text{SU-8}}$ = 4.02 GPa, $\upsilon_{\text{SU-8}}$ = 0.22, and $t_{\text{SU-8}}$ = 5 μm; (2) Y_{PZT} = 62.5 GPa, υ_{PZT} = 0.35, and t_{PZT} = 2 μm; and (3) Y_{PET} = 3 GPa, υ_{PET} = 0.4, and t_{PET} = 125 μm. The mechanical neutral plane is ~39 μm below the top surface. Therefore, the distance between the mechanical neutral plane and the middle of PZT thin film is about 33 μm.

The strain in the PZT active layer can be calculated by

$$\varepsilon = \frac{\delta}{r}$$

where r is the bending radius, and δ is the distance from the mechanical neutral plane. The calculated strain in the PZT thin film at bending radius of 1.61 cm is about 0.205 %.

Calculation for the energy conversion efficiency

The energy conversion efficiency (η %) is calculated as below definition:

$$\eta\ \% \equiv \frac{\text{Generated Electrical Energy } (E_{elec})}{\text{Stored Mechanical Energy } (E_{mech})} \times 100\ \%$$

Produced electrical energy:

The electrical energy loaded by the fixed resistance is calculated according to the following equation,

$$E_{elec} = \int [I(t)]^2 R\, dt$$

where I and R are current and resistance, respectively. The maximum power was estimated at about 50 MΩ. Therefore, the plot of I^2R can be obtained from the I-t curve, and the electrical energy in one cycle is calculated as

$$E_{elec} = 31.01\ \mu\text{J}$$

Mechanical energy at device level:

The E_{mech} can be calculated by the stored elastic energy (E_{elas}) of the PZT thin film in a single deformation. The elastic energy can be calculated by the below equation,

$$E_{elas} = \frac{1}{2} Y \varepsilon^2 V$$

where Y, ε, and V are elastic modulus, strain, and volume. The maximum strain of PZT thin film is about 0.205 %. Using the Young's modulus of PZT (~62.5 GPa) and the volume of PZT substrate (~0.002 cm^3), we can calculate

$$E_{elas} = 262.7\ \mu\text{J}$$

Therefore, the energy conversion efficiency can be approximately estimated as,

$$\eta\ \% = \frac{31.01\ \mu\text{J}}{262.7\ \mu\text{J}} \times 100\ \% \cong 11.8\ \%$$

Supplementary references

1. L. Kholkine, C. Wuetchrich, D. V. Taylor, and N. Setter, *Rev. Sci. Instrum.*, 1996, **67**, 1935-1941.

2. J. A. Christman, S.-H. Kim, H. Maiwa, J.-P. Maria, B. J. Rodriguez, A. Kingon, and R. J. Nemanich, *J. Appl. Phys.*, 2000, **87**, 8031.

3. H. Maiwa, N. Iizawa, D. Togawa, T. Hayashi, W. Sakamoto, M. Yamada, and S. Hirano, *Appl. Phys. Lett.*, 2003, **82**, 1760.

4. Y. Qi, J. Kim, T. D. Nguyen, B. Lisko, P. K. Purohit, and M. C. McAlpine, *Nano Lett.*, 2011, **11**, 1331-1336.